

Dear Author,

Please, note that changes made to the HTML content will be added to the article before publication, but are not reflected in this PDF.

Note also that this file should not be used for submitting corrections.



ELSEVIER

Contents lists available at ScienceDirect

International Journal of Pharmaceutics

journal homepage: www.elsevier.com/locate/ijpharm

Lipid-based nanoparticles containing cationic derivatives of PTA (1,3,5-triaza-7-phosphaadamantane) as innovative vehicle for Pt complexes: Production, characterization and *in vitro* studies

Rita Cortesi^{a,b,*}, Chiara Damiani^a, Laura Ravani^a, Lorenza Marvelli^c, Elisabetta Esposito^a, Markus Drechsler^d, Antonella Pagnoni^e, Paolo Mariani^f, Fabio Sforza^a, Paola Bergamini^b

^a Department of Life Sciences and Biotechnology, University of Ferrara, Ferrara, Italy

^b Nanopharmnet: The Italian Network of Pharmaceutical Nanotechnology and Nanomedicine, Italy

^c Department of Chemistry and Pharmaceutical Sciences, University of Ferrara, Ferrara, Italy

^d Macromolecular Chemistry II, University of Bayreuth, Germany

^e Department of Biochemistry and Molecular Biology, University of Ferrara, Ferrara, Italy

^f Department of Life and Environmental Sciences and CNISM, Polytechnic University of Marche, Ancona, Italy

ARTICLE INFO

Article history:

Received 12 May 2015

Received in revised form 6 July 2015

Accepted 7 July 2015

Available online xxx

Keywords:

PTA

Cationic lipid nanoparticles

Cisplatin

Antiproliferative activity

Pt complexes

ABSTRACT

The aliphatic phosphine PTA (1,3,5-triaza-7-phosphaadamantane) is a promising ligand for metal complexes designed and developed as innovative inorganic drugs.

In the present paper, an *N*-alkylated derivative of PTA, (PTAC₁₆H₃₃)X (X=I, C1, or X=PF₆, C2) and its platinum coordination complex *cis*-[PtCl₂(PTAC₁₆H₃₃)₂](PF₆)₂, C3, were considered as components of cationic lipid nanoparticles (CLNs). Particularly, CLN1, CLN2 and CLN3 were obtained by adding derivatives C1, C2 or C3 during nanoparticles preparation, while CLN2-Pt were obtained by treating preformed CLN2 with Pt(II). It was demonstrated that CLN1, CLN2 and CLN3 can be produced with technological conventional methods. However, among the two here proposed protocols, the one based on the treatment of preformed nanoparticles appears more advantageous as compared to the other since it allows a quantitative association yield of Pt. As determined by ICP-OES, a content of P and Pt 2.2-fold and 2.5-fold higher in CLN2-Pt than in CLN3 was evidenced. For the first time was demonstrated that properly functionalized preformed nanoparticles can be efficiently used to obtain a post production Pt(II) complex while maintaining a cytotoxic activity toward cultured cells. In fact, the antiproliferative activity shown by CLN3, CLN2-Pt on the three model cancer cell lines was substantially similar and comparable to that of complex C3 in dmsol solution. Thus *N*-alkylated-PTA derivatives in CLNs could be proposed as innovative biocompatible and water dispersible nanoparticles carrying lipophilic Pt complexes becoming an interesting and improved system with respect to dmsol solution.

© 2015 Published by Elsevier B.V.

1. Introduction

The aliphatic phosphine PTA (1,3,5-triaza-7-phosphaadamantane) (Fig. 1A) (Daigle et al., 1974) has been recently re-discovered and widely exploited in coordination chemistry due to its ability to coordinate a wide range of metals ions *via* phosphorus (Daigle, 1998; Phillips et al., 2004; Bravo et al., 2010). Moreover, being highly soluble in water, stable to oxidation, non-toxic and biocompatible, PTA is a promising ligand for metal-based drugs (Casini et al., 2008).

In specific conditions, PTA displays reactivity in all the positions of the cage structure. Notably, the alkylation of one nitrogen of PTA leads to a group of derivatives bearing a positive charge while maintaining the coordinative ability through the P-donor site (Fig. 1B) (García-Moreno et al., 2014; Wheate and Collins, 2003). When *N*-alkylated PTA derivatives are introduced as ligands in platinum or ruthenium complexes designed for anticancer activity, their cationic nature could be advantageous for the drug targeting. In fact, a positively charged drug is expected to be electrostatically attracted by its target, the polyanionic DNA7, resulting in higher speed and efficiency of action.

In this paper, we focus our attention on the *N*-hexadecyl-PTA derivative C1, containing a large lipophilic portion (i.e., C₁₆H₃₃) connected to the hydrophilic, positively charged PTA cage (Fig. 1C).

* Corresponding author at: Department of Life Sciences and Biotechnology, via Fossato di Mortara 19, 44121 Ferrara, Italy.
E-mail address: crt@unife.it (R. Cortesi).

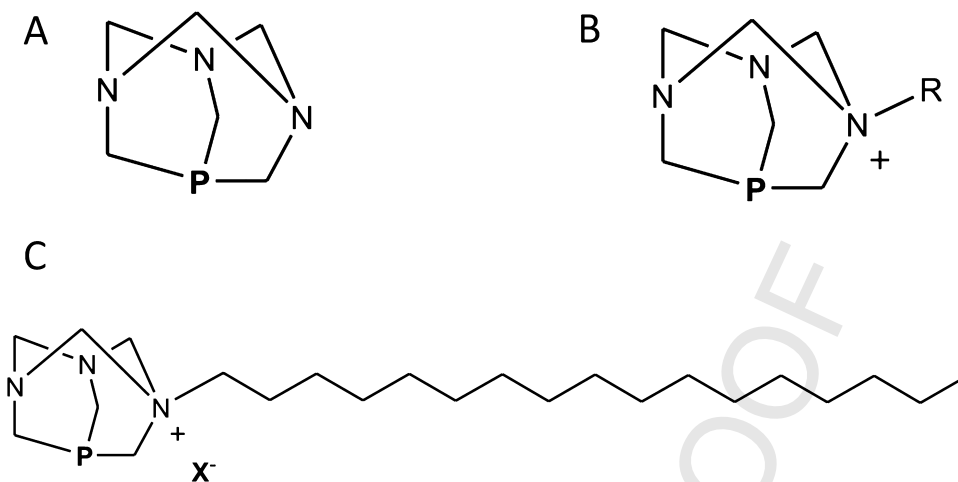


Fig. 1. Chemical structure of 1,3,5-triaza-7-phosphaadamantane PTA (A), N-alkylPTA (B) and N-HexadecylPTA⁺X⁻ (C).

The structure of the ligand, resembling a cationic species with amphiphilic surfactant properties, could influence the cell penetration and promote both the formulation and distribution of its metal complexes when they are used as drugs (Soussan et al., 2009). Unfortunately, notwithstanding the similarity of C1 to surfactants, the presence of a long aliphatic tail on PTA dramatically decreases its solubility in water. Thus, to overcome this drawback, we evaluated (whether lipid nanosystems, such as cationic lipid nanoparticles (CLN)) previously proposed as stable and industrial scalable nanosystems alternative to liposomes as cationic non-viral systems (Tabatt et al., 2004), could be considered as an alternative option for conveying C1 either as a free ligand or as a Pt complex (C3).

Indeed, it was proved that CLN and liposomes formulated from the same cationic lipids, demonstrated equipotent *in vitro* transfection efficiencies (Kaur and Slavcev, 2013). Hence, structural or compositional design changes of nanovectors may influence the outcome in relation with cell physiology, cell internalization pathways and transfection efficiency. Moreover CLN offer several advantages as compared to liposomes including improved physical stability, controlled release, ability to freeze dry and reconstitute, controllable particle size, low production cost and easy scale-up and manufacturing (Kaur and Slavcev, 2013).

The lipophilic N-alkylPTA⁺ derivative (PTAC₁₆H₃₃)⁺ has all the characteristics to be considered as a convenient component to produce CLNs, while allowing at the same time the metal coordination through its P-donor site.

Before coordination to platinum, it was necessary to convert the iodide salt (C1) to its hexafluorophosphate analogue (PTAC₁₆H₃₃)PF₆ (C2), in order to exclude the involvement of iodide in the coordination reactions of (PTAC₁₆H₃₃)⁺. The iodide ion was therefore exchanged with the non-coordinating anion PF₆⁻.

Summarizing, this study describes: (a) the preparation and characterization of cationic lipid nanoparticles loaded with (PTAC₁₆H₃₃)I (C1) or (PTAC₁₆H₃₃)PF₆ (C2) or with the platinum coordination complex *cis*-[PtCl₂(PTAC₁₆H₃₃)₂](PF₆)₂ (C3), (b) their ability to bind DNA and (c) their effect on cell proliferation of *in vitro* cultured human erythroleukemic K562 cells and human ovarian cancer cell lines, A2780 and SKOV3.

2. Materials and methods

2.1. Materials

The lipophilic PTA derivatives, N-hexadecyl-PTA iodide, (PTAC₁₆H₃₃)I, C1, and N-hexadecyl-PTA hexafluorophosphate,

(PTAC₁₆H₃₃)PF₆, C2, were synthesized and characterized by Bergamini et al., as previously reported (Bergamini et al., 2012). In Table 1 are summarized the structures and ³¹P NMR data of C1, C2 and C3.

Poloxamer 188, oxirane, methyl-, polymer with oxirane (75:30) was from BASF (Ludwigshafen, Germany). Miglyol 812, caprylic/capric triglyceride (tricaprylin) was from CREMER (Hamburg, Germany). All other materials and solvents were from Sigma-Aldrich S.r.l. (Milan, Italy).

2.2. Coordination of (PTAC₁₆H₃₃)PF₆ to Pt(II)-synthesis of C3

cis-[PtCl₂(PTAC₁₆H₃₃)₂](PF₆)₂, C3, was prepared by a method designed with the aim to minimize the presence of organic solvent and side-products alternative to the previously published method (Bergamini et al., 2012).

A solution of K₂PtCl₄ (0.26 g, 0.63 mmol) in 3 mL of water was added dropwise under stirring to a suspension of (PTAC₁₆H₃₃)PF₆ (0.66 g, 1.25 mmol) in 60 mL of CH₂Cl₂. The double phase system was stirred at room temperature for two hours. The organic phase, containing the product, was then separated and taken to complete dryness. The product was identified as *cis*-[PtCl₂(PTAC₁₆H₃₃)₂](PF₆)₂ (0.79 g, 0.6 mmol, yield 95%), by comparison of ¹H and ³¹P NMR data (Table 1) with those previously reported (Bergamini et al., 2012).

2.3. Preparation of N-alkylPTA⁺ containing CLNs

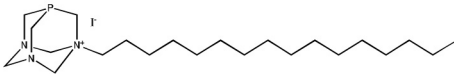
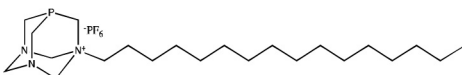
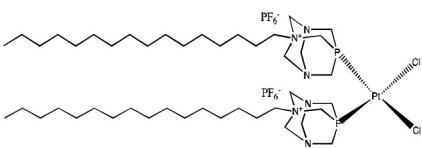
CLNs were prepared following already described procedures (Cortesi et al., 2014; Esposito et al., 2015, 2008). Briefly, 1 g of lipid mixture, constituted of tristearine, tricaprylin and C1 or C2 (6:3:1 w/w/w), was melted at 80 °C to give CLN1 and CLN2, respectively. To the fused lipid phase were added 19 mL of poloxamer 188 in aqueous solution (2.5% w/w). The obtained emulsion was ultrasonicated using a MicrosonTM, Ultrasonic cell Disruptor (Misonix Inc., NY, USA) at 6.75 kHz for 15 min and cooled down to room temperature. Afterwards, the obtained dispersions were stored at room temperature.

2.4. Preparation of Pt-containing CLNs

2.4.1. Preparation of CLN3

A sample of C3 (0.025 g = 1.9 × 10⁻⁵ mol) was dispersed in the lipid phase. Afterwards, CLN3 was obtained as described above for CLN1 and CLN2 (final volume 4.56 mL).

Table 1Chemical structure, name and ^{31}P NMR data in d_6 -dmsO solution and in CLNs of considered PTA derivatives.

Compound Name structure	^{31}P NMR (121.50 MHz)	
	d_6 -dmsO solution	CLN
<p>C1 (PTAC₁₆H₃₃)I</p> <p>N-hexadecyl(1,3,5-triaza-7-phosphaadamantane)iodide</p> 	-84.27 ppm (s), (Bergamini et al., 2012)	CLN1 -84.99 ppm (s)
<p>C2 (PTAC₁₆H₃₃)PF₆</p> <p>N-hexadecyl(1,3,5-triaza-7-phosphaadamantane) hexafluorophosphate</p> 	-84.27 ppm (s), -142.21 ppm (hept, $^1J_{\text{PF}}$ 707 Hz, PF ₆) (Bergamini et al., 2012)	CLN2 -85.00 ppm (s), -143.86 ppm (hept, $^1J_{\text{PF}}$ 705 Hz, PF ₆)
<p>C3 cis-[PtCl₂(PTAC₁₆H₃₃)₂]2PF₆</p> <p>[Bis(N-hexadecyl(1,3,5-triaza-7-phosphaadamantane)platinum dichloride] hexafluorophosphate</p> 	-42.68 ppm (s, $^1J_{\text{PtP}}$ 3381 Hz) -143.2 ppm (hept, $^1J_{\text{PF}}$ = 707 Hz, PF ₆)	CLN3 Not determined due to low P concentration
	-41.25 ppm (bs, $^1J_{\text{PtP}}$ 3400 Hz), -142.2 ppm (hept, $^1J_{\text{PF}}$ 707 Hz, PF ₆) (Bergamini et al., 2012)	CLN2-Pt -40.97 (bs, $^1J_{\text{PtP}}$ 3475 Hz), -144.00 (heptet, $^1J_{\text{PF}}$ 706 Hz, PF ₆)

The suspension was diluted 1:10 by volume in order to obtain an appropriate concentration for determining P and Pt final contents by ICP-OES analysis.

2.4.2. Preparation CLN2-Pt

4 mL of CLN2 containing 7.4×10^{-6} mol of C2 (93.1 mg/L determined by ICP-OES) were added to 1 mL of K₂PtCl₄ (1.53 mg/mL, 3.7×10^{-6} mol) and the mixture was stirred for 18 h. Afterwards, the content of P and Pt was determined by ICP-OES analysis.

2.5. Characterization of CLN: size, ζ potential and morphology

Submicron particle size analysis was performed using a Zetasizer 3000 PCS (Malvern Instr., Malvern, UK) equipped with a 5 mW helium neon laser with a wavelength output of 633 nm.

Glassware was cleaned of dust by washing with detergent and rinsing twice with water for injections. Measurements were made at 25 °C at an angle of 90°. Samples were diluted with MilliQ water to an adequate scattering intensity prior to measurement. The results are presented as an intensity weighted average value (z-ave) obtained from three measurements (10 runs each).

The ζ potential of CLNs was measured at room temperature by means of a Zetasizer nano ZSP (Malvern Instr., Malvern, UK) in purified water. Samples were poured in a polycarbonate capillary cell and analysed under a constant voltage after focusing with a 5 mW helium neon laser. The ζ potential value was obtained by means of M3-PALS technique. Each sample was measured three times and mean value and standard deviation (SD) were presented.

Morphological characterization of CLNs was performed by Cryo-TEM. Samples were vitrified as described by Esposito et al. (2008). A drop of dispersion was placed on a lacey carbonfilm-

coated copper TEM grid (200 mesh, Science Services). Most of the liquid was removed with blotting paper, leaving a thin film stretched over the carbon film holes. The specimens were put in a temperature-controlled freezing unit, subjected to freezing by immersion into liquid ethane (Zeiss Cryobox, Zeiss Microscopy GmbH, Göttingen, Germany) and cooled to approximately 90 K. This led to the formation of a thin vitrified film on the specimen. The temperature was monitored and kept constant in the chamber during all of the preparation steps. Frozen specimens are inserted into a cryo-transfer holder (CT3500, Gatan, München, Germany) and transferred to a Zeiss EM922 OMEGA EFTEM instrument. Examinations were carried out at around 90 K. The microscope operates at an acceleration voltage of 200 kV. Images were digitally recorded by a bottom-mounted CCD camera system (Ultrascan 1000, Gatan, München, Germany), combined and processed with a digital imaging processing system (Gatan Digital Micrograph 3.9 for GMS 1.4, München, Germany).

2.6. ^{31}P NMR characterization of CLN

NMR spectra were recorded using a Varian Gemini 300 MHz spectrometer (^1H at 300 MHz, ^{31}P at 121.50 MHz). The ^{31}P spectra were run with proton decoupling and are reported in ppm relative to an external 85% H_3PO_4 standard, with positive shifts downfield.

2.7. X-ray diffraction

X-ray diffraction experiments were performed using a 3.5 kW Philips PW 1830 X-ray generator (Philips, Eindhoven, The Netherlands) equipped with a homemade Guinier-type focusing camera operating in vacuum with a bent quartz crystal monochromator ($\lambda = 1.54 \text{ \AA}$). Diffraction patterns were recorded on a GNR analytical instruments imaging plate system (GNR Analytical Instruments Group, Novara, Italy). Samples were held in a tight vacuum cylindrical cell provided with thin Mylar windows. Diffraction data were collected at different temperatures, using a Haake F3 thermostat (ThermoHaake, Karlsruhe, Germany) with an accuracy of 0.1°C .

2.8. P and Pt determination in CLN by ICP-OES

P and Pt in CLNs were determined by Inductively Coupled Plasma Optical Emission Spectroscopy (ICP-OES) using an Optima 3100 XL spectrophotometer (PerkinElmer Italia srl, Milan, Italy) equipped with a PerkinElmer AS91 autosampler. The operating conditions used for quantification of P and Pt by ICP-OES are reported in Table 2.

2.9. Electrophoretic mobility of complexes between nanoparticles and DNA

CLNs were mixed with λ phage DNA in different +/- molar ratios (i.e., from 0.25:1 to 64:1) and incubated at 37°C for 5 min, then each sample was subjected to electrophoresis.

Table 2
Instrumental conditions for ICP-OES determination of P and Pt.

Parameter	P	Pt
Power (W)	1350	1350
Generator frequency (MHz)	40	40
Plasma, Ar flow rate (L min^{-1})	15	15
Nebulizer, Ar flow rate (L min^{-1})	0.65	0.65
Sample flow rate (mL min^{-1})	1.5	1.5
Read time (s)	Min 1–Max 5	Min 1–Max 5
Wavelength (nm)	P 213.617	Pt 214.423

Electrophoresis was carried out in 1% agarose gel at constant voltage (90 mV) for 40 min. The relative band migration was captured with Goldec 1000 (Bio-Rad, Segrate, Italy) photcamera after staining the gels with ethidium bromide.

2.10. Growth inhibition assays

Cell growth inhibition assays were carried out using human cells, namely erythroleukemic K562 and ovarian cancer cell lines A2780 and SKOV3 (Lozzio and Lozzio, 1975; Godwin et al., 1992; Mistry et al., 1992). Cells were maintained in RPMI 1640, supplemented with 10% calf serum, penicillin (100 U/mL), streptomycin (100 $\mu\text{g/mL}$) and glutamine (2 mM); the pH of the medium was 7.2 and the incubation was at 37°C in a 5% CO_2 atmosphere. Cells were routinely passed every three days at 70% of confluence; for the adherent cell lines, 0.05% trypsin-EDTA was used. The antiproliferative activity of compounds was tested with the MTT assay (Hansen et al., 1989). K562, A2780 or SKOV3 cells were seeded in triplicate in 96-well trays.

Stock solutions in dimethyl sulfoxide (dmsO) (10 mM) of C2, C3 and cisplatin were diluted in culture medium to final concentrations ranging from 5 to 50 μM of drug.

For all CLN-containing formulations, the requested concentrations were obtained from the original preparation (whose actual P and Pt contents were measured by ICP-OES) by appropriate dilutions with culture medium. The values of final concentrations are expressed as C2 concentration, and the Pt concentration (where present) is half.

The cells were exposed to the formulations for 72 h, then 25 μL of a 3-(4,5-dimethylthiazol-2-yl) 2,5-diphenyltetrazolium bromide solution (MTT) (12 mM) were added and incubated for 2 h. Afterwards, 100 μL of lysing buffer (50% DMF + 20% SDS, pH 4.7) were added to convert the MTT solution into a violet-colored formazane. After additional 18 h the solution absorbance, proportional to the number of live cells, was measured by spectrophotometer at 570 nm and converted into percentage of growth inhibition (Bergamini et al., 2013).

3. Results and discussion

3.1. Production and characterization of CLN

To produce CLN1, CLN2, and CLN3 (schematic representations in Fig. 2), C1, C2 or C3 were added to the main components of the formulation composed of a mixture of tristearine and tricaprilyn as described in the experimental section. It is to be underlined that the presence of pure tristearin allows the achievement of stable and homogenous dispersions, free from aggregates (Esposito et al., 2008).

After production, CLNs were subjected to the evaluation of P and Pt contents by means of ICP-OES analysis and the results are reported in Table 3.

The content of P (proportional to the content of included C2, 2 phosphorus per mole of phosphine, including PF_6^- anion) was firstly measured in CLN2. It was found that the final incorporation of P was 110 mg/L, that is, 16.3% of the calculated amount of P (675 mg/L).

CLN2-Pt were obtained through the coordination of Pt to the phosphine ($\text{PTAC}_{16}\text{H}_{33}\text{PF}_6$) included in CLN2. The ligand C2 is present in CLN2 presumably exposing the hydrophilic group (PTAN^+) that bears the coordinating site (phosphorus atom) on the nanoparticle surface. The coordination was obtained by mixing a suspension of preformed CLN2 with an aqueous solution of K_2PtCl_4 .

Particularly, for CLN2-Pt the amount of P was 91.7 mg/L (calc. $7.4 \times 10^{-6} \times 2/0.005 \text{ L} \times 31 = 91.8 \text{ mg/L}$) and Pt was 139 mg/L (calc.

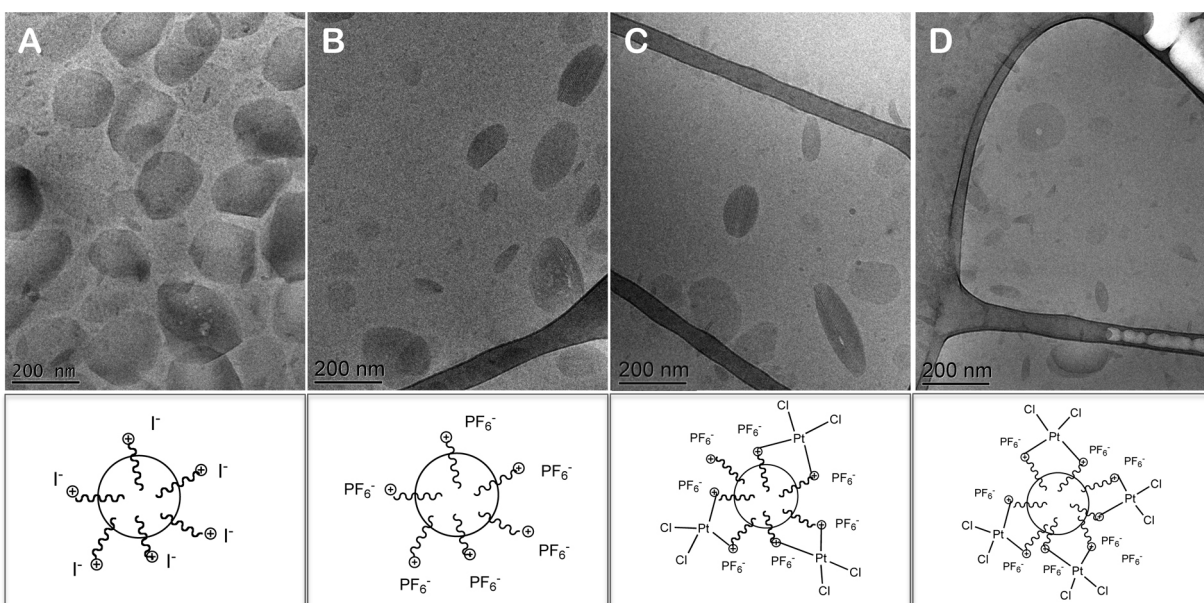


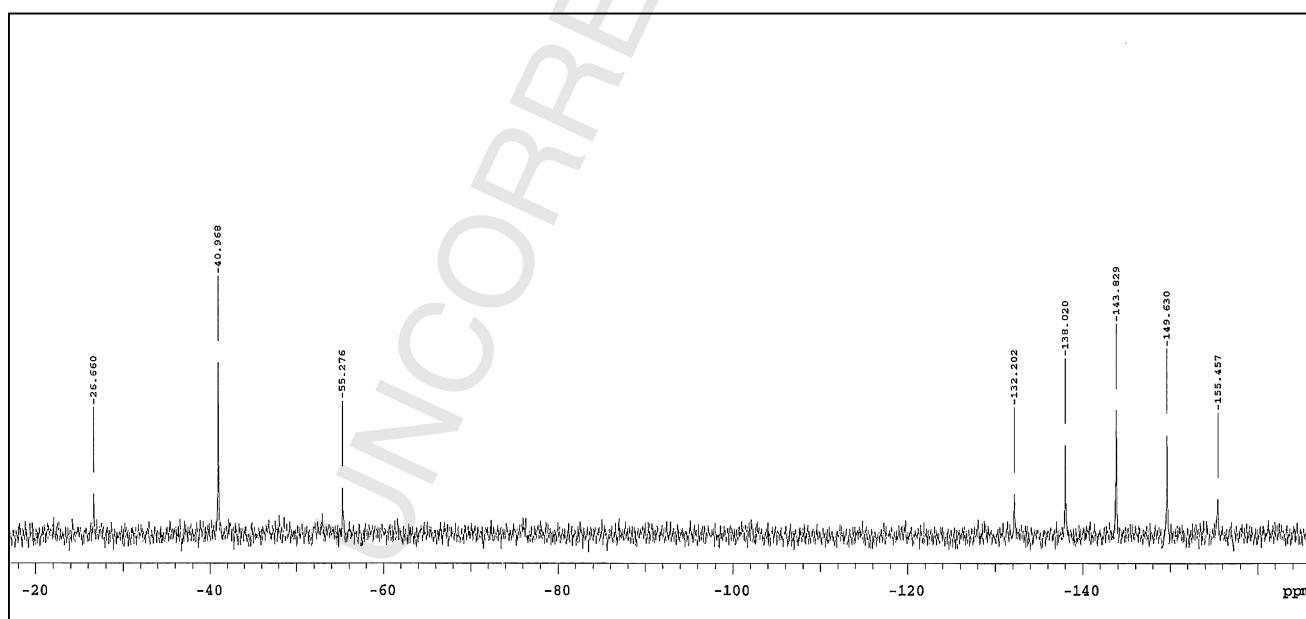
Fig. 2. Schematic representation and cryo-TEM photographs of the CLNs studied in the present paper. Panel A: CLN1; Panel B: CLN2. Panel C: CLN2-Pt. Panel D: CLN3. Bar represents 0.2 μm .

Table 3

P and Pt concentration (mg/L) and percentage of presence in CLNs as determined by ICP-OES.

	P ICP-OES/calc. (%)	Pt ICP-OES/calc. (%)	Pt/P mass ratio ICP-OES/calc.
CLN2	110/675 (16.3%)	–	–
CLN3	41.5/496 (8.4%)	54.2/780 (6.9%)	1.31/1.57
CLN2-Pt	91.7/91.8 (99.9%)	139/144 (96.5%)	1.55/1.57

Concentrations in mg/L in nanoparticles as determined by ICP-OES/concentrations in mg/L used for nanoparticles production. In brackets percentage of loading.



$^{31}\text{P}\{^1\text{H}\}$ NMR (121.5 MHz, 25°C):

δ -40 ppm (s) ($^1J_{\text{PtP}} = 3400$ Hz), -143.0 ppm (ept, $^1J_{\text{PF}_6} = 707.5$ Hz, PF_6^-)

Fig. 3. ^{31}P NMR spectrum of CLN2-Pt.

$3.7 \times 10^{-6}/0.005 \text{ L} \times 195 = 144 \text{ mg/L}$) corresponding to an incorporation percentage of 99.9% and 97.9%, respectively. The mass ratio Pt/P measured by ICP-OES was 1.55 (calc. 1.57).

The formation of the complex was demonstrated by comparison of ^{31}P NMR data (-40.97 ppm , $^1J_{\text{PtP}} 3475 \text{ Hz}$, -143.0 ppm hept, $^1J_{\text{PtF}} 707 \text{ Hz}$, PF_6^- , Fig. 3) with those found for complex 3, in dmsol solution (-39.6 ppm , $^1J_{\text{PtP}} = 3422 \text{ Hz}$, -143.0 ppm hept, $^1J_{\text{PF}} = 707.5 \text{ Hz}$, PF_6^-) (Table 1).

In the case of CLN3, the P concentration determined by ICP-OES was 41.5 mg/L (calc. on the initial 0.025 g of C3: 496 mg/L) whereas that of Pt was 54.2 mg/L (calc. on initial 0.025 g of C3: 780 mg/L) corresponding to an incorporation percentage of 8.4 and 6.9 for P and Pt, respectively.

The mass ratio Pt/P measured by ICP-OES was 1.31 (calc. 1.57) (Table 3).

In this case, the acquisition of ^{31}P NMR data was prevented by the low concentration of phosphorus.

From the results reported above, it is clearly evident that a large amount of phosphine C2 is lost during the preparation of CLN2, but the loaded aliquot, although small (16.3%), is totally and efficiently available for the formation of Pt complex (97.9% in CLN2-Pt). This result is quite interesting if we consider the difference in terms of cost-to-value ratio between phosphine C2 and platinum.

Moreover, comparing the figures of Pt-containing nanoparticles reported in Table 3, namely CLN2-Pt and CLN3, a loss in the amount of the species to be loaded (phosphine C2 and complex C3, respectively) is evident in both cases, which can possibly be ascribed to the technical procedure used during (for) their preparation.

However, in terms of recovery of Pt (Pt recovery), it should be underlined that the treatment of preformed CLN2 with K_2PtCl_4 appears much more advantageous as compared to the production of CLN3, since it allows a quantitative yield of Pt inclusion. Moreover, it is worth noting that the final concentration of P and Pt is higher in CLN2-Pt than in CLN3 (2.2- and 2.5-fold, respectively).

These observations indicate the method proposed for CLN2-Pt as the most convenient to prepare Pt-containing nanoparticles.

All the CLNs obtained were characterized in terms of morphology, size and charge.

Fig. 2 shows cryo-transmission electron microscopy (cryo-TEM) photographs of the produced CLNs. It should be underlined that, due to the presence of phosphorus, the samples were very radiation-sensitive on the surface; therefore, the images appear a bit noisy, unclear and hidden. However, it is possible to appreciate that CLNs are characterized by the presence of three-dimensional particles projected in a two-dimensional way displaying ovoid platelet-like particles and needle-like structures. The calculated thickness of nanoparticles is around 10 nm .

In particular, it is possible to note in CLN1 (panel A) some particles that internally show vesicular shapes probably due to the presence of the oily lipid. These structures can be visible also in CLN2 (panel B) and CLN2-Pt (panel C). Moreover, both CLN2's show

a more inhomogeneous population as compared to CLN1, characterized in some cases by a lamellar ultrastructure. In addition, the presence of the coordinated Pt(II) does not seem to influence CLN's morphology. Concerning CLN3 (panel D), no appreciable morphological differences are evident.

Table 4 summarizes the results concerning size and ζ potential of the produced CLN. From the analysis of these data, it can be inferred, that, in general, the presence of C1 or C2 induce a slight decrease in the mean diameter of nanoparticles as compared to nanoparticles without *N*-alkylPTA derivative (i.e., plain nanoparticles). Moreover, as also visualized by cryo-TEM, the coordination of Pt(II) by CLN2 does not influence the mean size. Indeed, the size is almost the same for both colloidal systems, being $185.15 \pm 4.38 \text{ nm}$ (P.I. 0.30) for CLN2 and $188.13 \pm 3.58 \text{ nm}$ (P.I. 0.25) for CLN2-Pt. Lastly, CLN3 shows a slight increase in the mean diameter as compared to CLN2. This result was expected because of the higher steric hindrance of C3 with respect to that of C2. Finally, it should be underlined that CLN1 and CLN2 maintain their dimensions almost unchanged at least for up to six months, while the Pt-containing CLNs tend to precipitate after a couple of days, probably due to the high Pt atomic weight (data not shown).

In order to obtain information about the charge of the particles, the ζ potential of CLN1 and CLN2 was measured. From data reported in Table 4, it is evident that both CLN1 and CLN2 show a positive charge as compared to plain nanoparticles. However, the type of counterion seems to influence the entity of the charge. In fact, CLN1 (whose counterion is I^-) are characterized by a ζ potential of $+19.8 \pm 0.4 \text{ mV}$, while CLN2 (whose counterion is PF_6^-) show a ζ potential of $+2.3 \pm 0.3 \text{ mV}$. Moreover, as expected, the presence of Pt does not influence the surface charge of the nanoparticles that show a value of ζ potential in the range of neutrality.

X-ray diffraction was used to investigate the inner structural organization of CLNs. Experiments were performed on CLN1, taken as an example, as a function of temperature (namely 25°C , 37°C and 45°C) and the results are reported in Fig. 4. The low-angle diffraction region shows a large peak, indicating an inner lamellar order. The diffraction patterns, measured at the three temperatures, are superimposable, suggesting a strong structural stability.

3.2. Binding migration studies of CLN

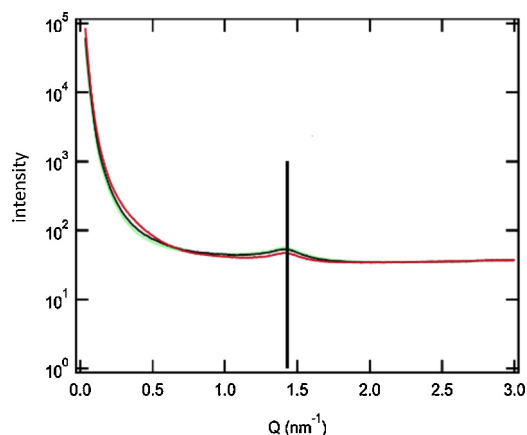
Notwithstanding the low values of ζ potential, a study to evaluate the interaction occurring between DNA and the produced CLNs was performed. CLNs were incubated with the λ -phage DNA to different final charge $+/-$ molar ratios (see Fig. 5) and subjected to electrophoresis. The high-molecular-weight complexes formed by the making of inter-nanoparticle bridges between CLNs and λ DNA molecules induce a retard in the DNA migration during electrophoresis (Sternberg et al., 1994; Cortesi et al., 1996). From the analysis of Fig. 5 it emerges that, when incubated with CLN2 (Fig. 5A), the λ DNA migrates with the same speed of the control,

Table 4
Size and ζ potential of the produced CLNs.

CLN	Z average (nm)	P.I.*	Analysis by volume				ζ potential (mV)
			Peak 1 area (%)	Mean diam 1 (nm)	Peak 2 area (%)	Mean diam 2 (nm)	
Plain	202.95 ± 0.51	0.19 ± 0.02	70.2 ± 8.8	113.7 ± 12.0	29.8 ± 8.2	309.3 ± 6.9	-20.0 ± 0.6
CLN1	194.54 ± 3.22	0.27 ± 0.03	86.7 ± 7.1	84.7 ± 17.0	13.4 ± 7.1	261.3 ± 21.5	$+19.8 \pm 0.4$
CLN2	185.15 ± 4.38	0.30 ± 0.02	76.7 ± 4.3	98.8 ± 10.5	23.4 ± 4.3	361.9 ± 16.2	$+2.3 \pm 0.3$
CLN2-Pt	188.13 ± 3.58	0.25 ± 0.01	92.9 ± 0.1	150.7 ± 1.1	8.1 ± 0.07	287.5 ± 2.26	$+1.5 \pm 0.3$
CLN3	207.73 ± 1.17	0.26 ± 0.03	90.3 ± 6.4	105.9 ± 22.1	9.7 ± 6.4	324.7 ± 57.1	$+3.1 \pm 0.5$

Data represent the mean of three independent experiments \pm SD.

* P.I., polydispersity index.



Q8 **Fig. 4.** X-ray diffraction profiles for CLN1 performed at 25 °C (green), 37 °C (black) and 45 °C (red). (For interpretation of the references to color in this figure legend, the reader is referred to the web version of this article.)

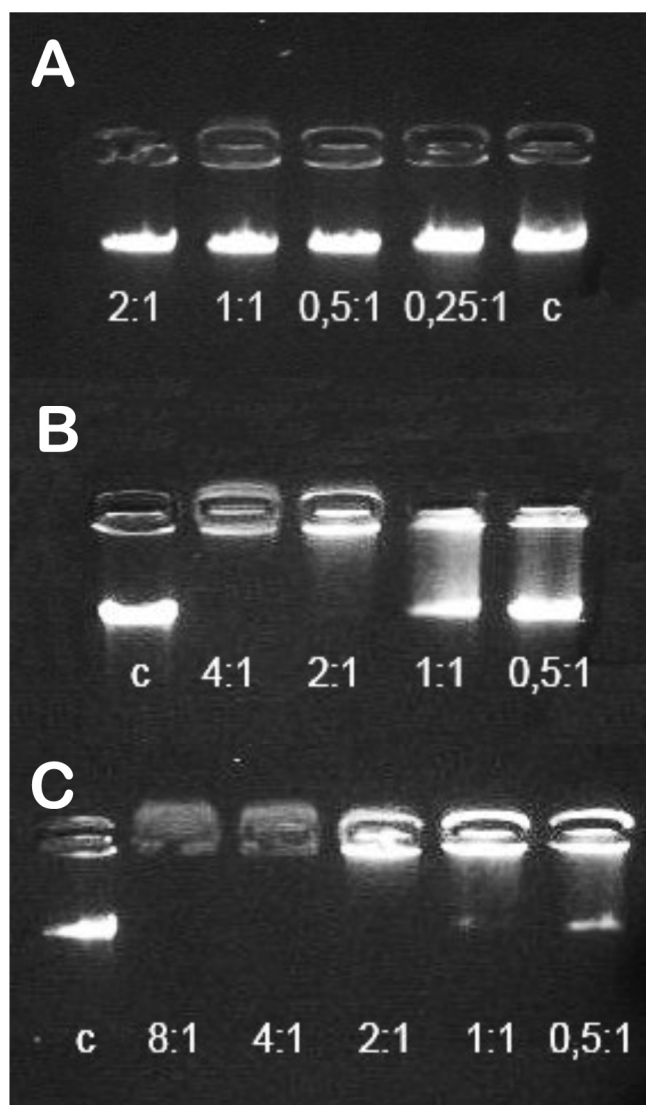


Fig. 5. Effect of cationic complexation on λ -phage DNA electrophoretic migration. For each type of CLN the used \pm molar charge ratio between CLNs and DNA was indicated. c = free DNA. Panel A: CLN2. Panel B: CLN2-Pt. Panel C: CLN3.

thus indicating that complexes with DNA are not formed. On the other hand, it is evident that when λ DNA is incubated with CLN2-Pt (Fig. 5B) or CLN3 (Fig. 5C), stable complexes are obtained. Particularly, as seen from the trail left by the migration of DNA, for CLN2-Pt the complex starts to be formed at molar \pm charge ratios of 0.5:1 and 1:1 and is completed at molar \pm charge ratios of 2:1. In addition, it can be underlined that the strength of complex formation is higher in the case of CLN3 with respect to CLN2-Pt, being the charge \pm molar ratio between CLN and DNA 1:1 and 2:1, respectively. Taking into account both the low ζ potential and the inability of CLN2 to form complexes, these results clearly indicate that the presence of coordinated Pt in CLN2-Pt and in CLN3 can play a decisive role in the interaction with DNA.

3.3. In vitro assays of antiproliferative activity

Recently, nanoparticulate self-assemblies of lipid surfactants in aqueous media received much attention as safe drug delivery systems (Svilenov and Tzachev, 2014). Lipid nanocarriers can improve safety of product by solubilizing and stabilizing drug molecules, targeting them to the site of action and/or changing the pharmacokinetics of drugs since lipid based nanomedicines, after systemic administration, distribute differently in the body and interact differently with biological components at cellular/subcellular level compared to formulations of free drug molecules (Svilenov and Tzachev, 2014). CLN contain a cationic lipid/surfactant in their composition and are mainly used for gene delivery or for drug delivery for special routes (Souto et al., 2010). In comparison to traditional SLN, CLNs have greater affinity to serum proteins (Lv et al., 2006) and cell membranes possibly facilitating the interaction with cellular receptors and subsequent uptake (Doktorovová et al., 2014; Lin et al., 2013). Concerning CLNs it has to be underlined that the toxicity of bulk excipients is a good starting point in the evaluation of toxicity and safety. Notably, most of the excipients used in the preparation of SLN can be found listed in many Pharmacopoeias, in Codex General Standard for Food Additives issued by FAO/WHO or in the current European and US cosmetics regulations (Svilenov and Tzachev, 2014). Lipids are physiological compounds characterized by high safety profile and high LD50 values. Most of them being components of food sources naturally present metabolic pathways for their degradation. Surfactants may be a larger issue in terms of toxicity evaluation since most of them are synthetic or semisynthetic products and not all find application in pharmaceutical products. Although the bulk excipients may have high LD50 values and GRAS status a detailed examination on the cytotoxicity of the final formulations should be performed. Proof of the safety of SLN can be found in the scientific literature (Svilenov and Tzachev, 2014; Vighi et al., 2012). Furthermore, SLN with suitable composition have shown to be well tolerated *in vitro*, as well as after *in vivo* administration in mice and rats (Muller et al., 1997; Joshi and Muller, 2009). It is worth mentioning that using GRAS substances with suitable amounts in CLN lead to an advantageous toxicity profile.

In order to obtain information about the potential antiproliferative activity of CLNs, some *in vitro* assays were performed as described in the experimental section. Particularly, human erythroleukemic K562 and ovarian cancer cell lines A2780 and SKOV3 were used. Cisplatin was employed as a control for both the cisplatin-sensitive A2780 and cisplatin-resistant SKOV3 cells. Untreated cells were used as a negative control. The results reported in Fig. 6 and in Table 5 express the average of three independent experiments conducted in triplicate.

The reliability of the tests performed is confirmed both by the behaviour of the CLN-untreated controls, whose proliferation is not inhibited for the duration of the test and also by the value of the

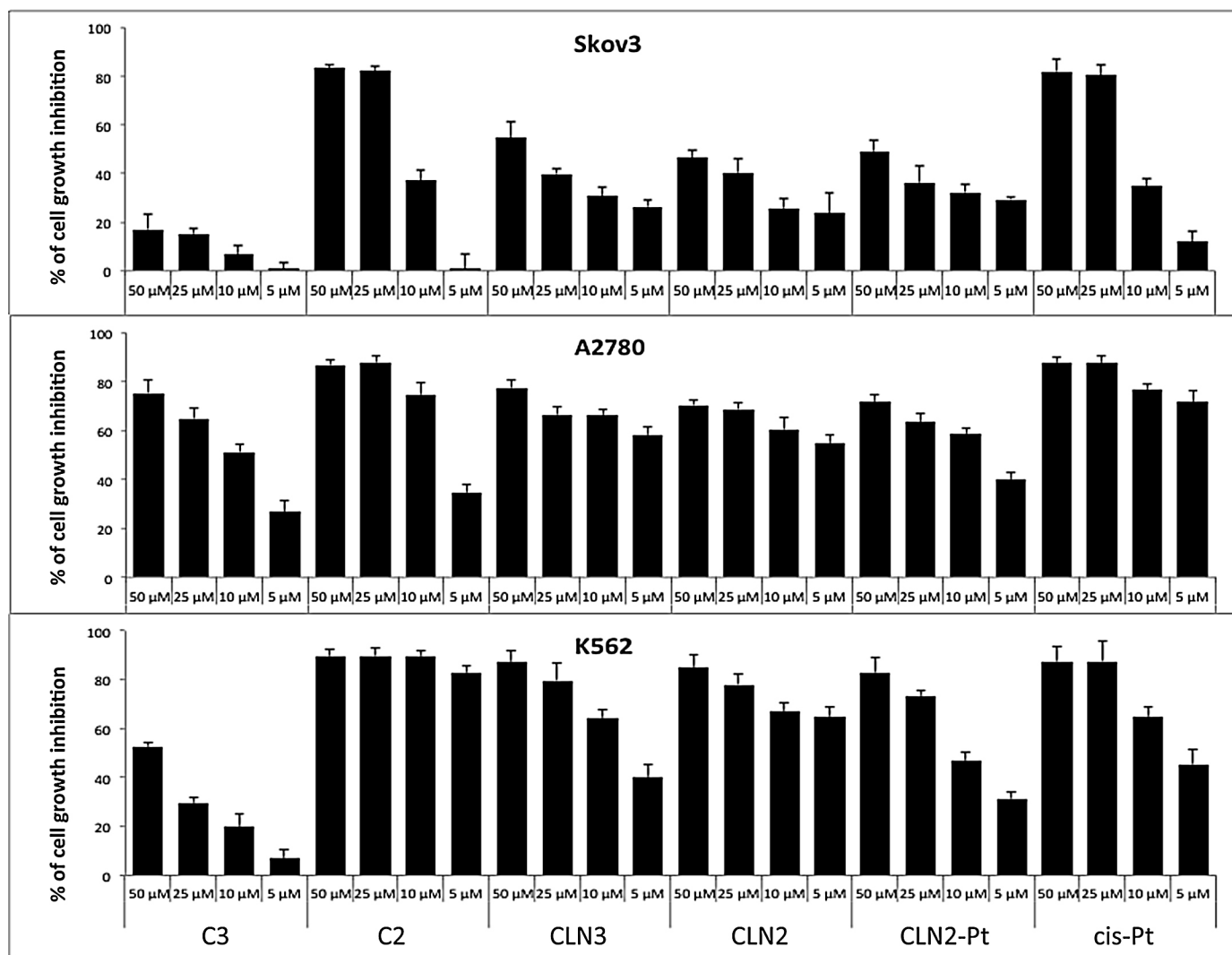


Fig. 6. *In vitro* antiproliferative effect of the different CLNs. Determinations were performed after 5 days of cell culture. Data represent the % of cell number/ml compared to untreated control cells. Panel A: human erythroleukemic K562 cells. Panel B: human ovarian cancer cells A2780. Panel C: human ovarian cancer cells SKOV3. The reported results are the average of three independent experiments, SD \leq 7%.

Table 5
IC₅₀ values of Pt-containing compounds and CLNs on human cancer cells.

	IC ₅₀ (μM)		
	SKOV3	A2780	K562
cis-Pt	15 ± 1	2 ± 1	6 ± 2
C2	14 ± 1	5 ± 2	3 ± 1
C3	>50	10 ± 3	26 ± 2
CLN2	>50	4 ± 1	3 ± 1
CLN2-Pt	>50	8 ± 3	14 ± 2
CLN3	43 ± 3	4 ± 2	6 ± 2

IC₅₀ are determined from the dose/response curves using MTT assay. Results are expressed as the mean of three independent experiments ± SD.

concentration of cisplatin causing a 50% inhibition of cell growth (IC₅₀) (Table 5) that confirms the resistance of the cell line SKOV3.

It should be underlined that plain nanoparticles show no toxicity if added in a quantity below 1% of the total volume of the cell culture, while, when added in percentages ranging between 2.5% and 5%, they show moderate toxicity towards all three cell lines, possibly due to the presence of poloxamer used as surfactant (Cortesi et al., 2012). Indeed, it is well known that, in general, uncharged lipid nanoparticles do not exhibit cytotoxic effects *in*

vitro up to concentrations of 2.5% lipid (Schubert and Muller-Goymann, 2005); whilst, for instance, lipid concentrations higher than 10% have shown a viability of 80% in cultured human granulocytes (Muller et al., 1996). Moreover, since the use of biocompatible fatty acids does not lead to toxic effects resulting from lipid nanoparticles degradation products, the cytotoxicity of lipid nanoparticles can be attributable to the presence of emulsifiers and surfactants used in their production (Tabatt et al., 2004; Heydenreich et al., 2003). In the present study the *N*-alkylPTA derivatives C1 and C2 are used for the preparation of CLNs with the aim to obtain the surfactant activity and positive charge necessary to form the initial emulsion and to provide the superficial charge for the interaction with DNA. Many studies in literature report that the presence of one-tailed cationic lipid in lipid nanoparticles is critical with respect to cell toxicity and a high toxicity is normally observed (Tabatt et al., 2004; Olbrich et al., 2001). To prevent the risk of toxicity due to the presence of *N*-alkylPTA derivatives cationic surfactant, its concentration in the formulation has been maintained as low as possible.

From the analysis of data reported in Fig. 6, it is evident that the compound C2, when used either free or included in nanoparticles (CLN2), shows small IC₅₀ values on A2780 and K562 cells (i.e., 5 μM and 3 μM for C2 and 4 μM and 3 μM for CLN2).

On the other hand, the platinum complex C3 was found inactive on SKOV3 ($IC_{50} > 50 \mu M$) and poorly active against A2780 and K562 cells (IC_{50} 10 and 26 μM , respectively), and showed generally a lower activity as compared to its free ligand C2. However, the activity shown by C2 can be ascribed to an inhibition mechanism unrelated to that of platinum-containing species, which is repressed when C2 is coordinated to platinum, while it is conserved when C2 is included in CLN2. Taking into account the antiproliferative activity shown by CLN2 (see Table 5 and Fig. 6), this consideration is also supported by the inability of CLN2 to bind DNA as observed above (see Fig. 5).

When Pt is conveyed by nanoparticles, such as CLN2-Pt or CLN3, its antiproliferative activity on A2780 and K562 is only slightly improved with respect to its free form C3 in dmsol solution, suggesting that the nanoparticles can be proposed as an inert vehicle.

This apparently negligible result is quite interesting if we consider that Pt complexes with lipophilic ligands are so poorly soluble in water that they need to be solubilized in dmsol in order to be tested or administrated. While dmsol has long been widely accepted as a solvent for this purpose, questions have been recently raised regarding its safety/suitability/effectiveness (Hall et al., 2014; Kelava et al., 2011; Galvao et al., 2014). Thus, the possibility to use innovative biocompatible and water dispersible nanoparticles carrying lipophilic Pt complexes could be proposed as an interesting and improved system as compared to the dmsol solution.

Another interesting aspect to underline is that the antiproliferative activity of both CLN2-Pt and CLN3 (used at the same concentration of Pt) against the three different cell lines is comparable. For instance, CLN3 show an IC_{50} of 4.0 μM and 6.0 μM against A2780 and K562 cells, respectively, while CLN2-Pt display an IC_{50} of 8 μM and 14 μM against A2780 and K562 cells, respectively.

Taken together these results indicate that the different method of preparation does not affect appreciably the action of Pt complexes. Particularly, the two synthetic routes to obtain Pt-containing CLNs, that is, preformed complex C3 included in nanoparticles giving CLN3 or ligand C2 pre-included in nanoparticles (CLN2) and then treated with K_2PtCl_4 to give CLN2-Pt, are equivalent in terms of product performance and therefore can both be exploited for best user convenience.

4. Conclusions

From the results presented in this study, the following conclusions can be drawn.

Cationic lipid nanoparticles, namely CLN1, CLN2 and CLN3, containing $(PTAC_{16}H_{33})I$ or $(PTAC_{16}H_{33})PF_6$ or the platinum complex $cis-[PtCl_2(PTAC_{16}H_{33})_2](PF_6)_2$, respectively, can be produced with technological conventional methods. However, it was here demonstrated that, of the two proposed protocol methods, the one based on the treatment of preformed nanoparticles, leading to CLN2-Pt, appears more advantageous as compared to the other, leading to CLN3, since it allows a quantitative association yield of Pt.

CLN3 and CLN2-Pt, checked in terms of physical properties showed some morphologic differences. Moreover, as determined by ICP-OES, a content of P and Pt 2.2-fold and 2.5-fold higher in CLN2-Pt than in CLN3 was evidenced.

Differently from previously published patents concerning the production of solid lipid nanoparticles containing platinum compounds (Gasco et al., 2008), it was demonstrated for the first time that properly functionalized preformed nanoparticles can be efficiently used to obtain a post production Pt(II) complex while maintaining a cytotoxic activity toward cultured cells. In fact, the

antiproliferative activity shown by CLN3, CLN2-Pt on the three model cancer cell lines was substantially similar and comparable to that of complex C3 in dmsol solution. This means that the antiproliferative activity of C3 is not affected by its inclusion in CLNs and therefore these nanoparticles can be proposed as an inert vehicle.

Moreover, these results allowed us to suggest the use of N-alkylated-PTA derivatives in CLNs as innovative biocompatible and water dispersible nanoparticles carrying lipophilic Pt complexes as an interesting and improved system with respect to dmsol solution. We further intend to explore the possibility to extend this method to other poorly water-soluble lipophilic Pt complexes bearing a positive charge.

Acknowledgement

The authors are grateful to Dr. Paolo Formaglio for the acquisition of NMR spectra.

References

- Bergamini, P., Marvelli, L., Marchi, A., Vassanelli, F., Fogagnolo, M., Formaglio, P., Bernardi, T., Gavioli, R., Sforza, F., 2012. Platinum and ruthenium complexes of new long-tail derivatives of PTA (1,3,5-triaza-7-phosphaadamantane): synthesis, characterization and antiproliferative activity on human tumoral cell lines. *Inorg. Chim. Acta* 391, 231–238.
- Bergamini, P., Marvelli, L., Marchi, A., Bertolasi, V., Fogagnolo, M., Formaglio, P., Sforza, F., 2013. New PTA (1,3,5-triaza-7-phosphaadamantane) derivatives associating zwitterionic structure and coordinative ability. *Inorg. Chim. Acta* 398, 11–18.
- Bravo, J., Bolaño, S., Gonsalvi, L., Peruzzini, M., 2010. Coordination chemistry of 1,3,5-triaza-7-phosphaadamantane (PTA) and derivatives. Part II. The quest for tailored ligands, complexes and related applications. *Coord. Chem. Rev.* 254, 555–607.
- Casini, A., Gabbiani, C., Sorrentino, F., Rigobello, M.P., Bindoli, A., Geldbach, T.J., Marrone, A., Re, N., Hartinger, C.G., Dyson, P.J., Messori, L., 2008. Emerging protein targets for anticancer metallodrugs: inhibition of thioredoxin reductase and cathepsin B by antitumor ruthenium(II)-arene compounds. *J. Med. Chem.* 51, 6773–6781.
- Cortesi, R., Esposito, E., Menegatti, E., Gambari, R., Nastruzzi, C., 1996. Effect of cationic liposome composition on their *in vitro* cytotoxicity and protective effect on carried DNA. *Int. J. Pharm.* 139, 69–78.
- Cortesi, R., Bergamini, P., Ravani, L., Drechsler, M., Costenaro, A., Pinotti, M., Campioni, M., Marvelli, L., Esposito, E., 2012. Long-chain cationic derivatives of PTA (1,3,5-triaza-7-phosphaadamantane) as new components of potential non-viral vectors. *Int. J. Pharm.* 431, 176–182.
- Cortesi, R., Campioni, M., Ravani, L., Drechsler, M., Pinotti, M., Esposito, E., 2014. Cationic lipid nanosystems as carriers for nucleic acids. *New Biotechnol.* 31, 44–54.
- Daigle, D.J., Pepperman Jr., A.B., Vail, S.L., 1974. Synthesis of a monophosphorus analog of hexamethylenetetramine. *J. Heterocycl. Chem.* 11, 407–408.
- Daigle, D.J., 1998. 1,3,5-Triaza-7-phosphatricyclo[3.3.1.1^{3,7}]decane and derivatives. *Inorg. Synth.* 32, 40–45.
- Doktorovová, S., Santos, D.L., Costa, I., Andreani, T., Souto, E.B., Silva, A.M., 2014. Cationic solid lipid nanoparticles interfere with the activity of antioxidant enzymes in hepatocellular carcinoma cells. *Int. J. Pharm.* 471, 18–27.
- Esposito, E., Fantin, M., Marti, M., Drechsler, M., Paccamiccio, L., Mariani, P., Sivieri, E., Lain, F., Menegatti, E., Morari, M., Cortesi, R., 2008. Solid lipid nanoparticles as delivery systems for bromocriptine. *Pharm. Res.* 25, 1521–1530.
- Esposito, E., Boschi, A., Ravani, L., Cortesi, R., Drechsler, M., Mariani, P., Moscatelli, S., Contado, C., Di Domenico, G., Nastruzzi, C., Giganti, M., Uccelli, L., 2015. Biodistribution of nanostructured lipid carriers: a tomographic study. *Eur. J. Pharm. Biopharm.* 89, 145–156.
- Galvao, J., Davis, B., Tilley, M., Normando, E., Duchon, M.R., Cordeiro, M.F., 2014. Unexpected low-dose toxicity of the universal solvent DMSO. *FASEB J.* 28, 1–14.
- García-Moreno, E., Gascón, S., Atrián-Blasco, E., Rodríguez-Yoldi, M.J., Cerrada, E., Laguna, M., 2014. Gold(I) complexes with alkylated PTA (1,3,5-triaza-7-phosphaadamantane) phosphanes as anticancer metallodrugs. *Eur. J. Med. Chem.* 79, 164–172.
- Gasco, M.R., Gasco, P., Bernareggi, A., 2008. Nanoparticle formulations of Platinum compounds, US Pat., 0038 371 A1.
- Godwin, A.K., Meister, A., O'Dwyer, P.J., Huang, C.S., Hamilton, T.C., Anderson, M.E., 1992. High resistance to cisplatin in human ovarian cancer cell lines is associated with marked increase of glutathione synthesis. *Proc. Natl. Acad. Sci. U. S. A.* 89, 3070–3074.
- Hall, M.D., Telma, K.A., Chang, K.-E., Lee, T.D., Madigan, J.P., Lloyd, J.R., Goldlust, I.S., Hoeschele, J.D., Gottesman, M.M., 2014. Say no to DMSO: dimethylsulfoxide inactivates cisplatin, carboplatin, and other platinum complexes. *Cancer Res.* 74, 3913–3922.

- Hansen, M.B., Nielsen, S.E., Berg, K.J., 1989. Re-examination and further development of a precise and rapid dye method for measuring cell growth/cell kill. *J. Immunol. Methods* 119, 203–210.
- Heydenreich, A.V., Westmeier, R., Pedersen, N., Poulsen, H.S., Kristensen, H.G., 2003. Preparation and purification of cationic solid lipid nanospheres – effects on particle size, physical stability and cell toxicity. *Int. J. Pharm.* 254, 83–87.
- Joshi, M.D., Muller, R.H., 2009. Lipid nanoparticles for parenteral delivery of actives. *Eur. J. Pharm. Biopharm.* 71, 161–172.
- Kaur, T., Slavcev, R., 2013. Solid lipid nanoparticles: tuneable anti-cancer gene/drug delivery systems. In: Wei, M., Good, D. (Eds.), *Novel Gene Therapy Approaches*. Intech Available from: <http://www.intechopen.com/books/novel-gene-therapy-approaches/solid-lipid-nanoparticles-tuneable-anti-cancer-gene-drug-delivery-systems>.
- Kelava, T., Javar, I., Culo, F., 2011. Biological actions of drug solvents. *Period. Biol.* 113, 311–320.
- Lin, Y., Suwayeh, Al-, Leu, S., Shen, Y., Fang, F.J., 2013. Squalene-containing nanostructured lipid carriers promote percutaneous absorption and hair follicle targeting of diphenylprone for treating alopecia areata. *Pharm. Res.* 30, 435–446.
- Lv, H., Zhang, S., Wang, B., Cui, S., Yan, J., 2006. Toxicity of cationic lipids and cationic polymers in gene delivery. *J. Control. Release* 114, 100–109.
- Lozzio, C.B., Lozzio, B.B., 1975. Human chronic myelogenous leukemia cell line with positive Philadelphia chromosome. *Blood* 45, 321–334.
- Mistry, P., Kelland, L.R., Loh, S.Y., Abel, G., Murrer, B.A., Harrap, K.R., 1992. Comparison of cellular accumulation and cytotoxicity of cisplatin with that of tetraplatin and amminedibutyratochloro(cyclohexylamine) platinum(IV) (JM221) in human ovarian carcinoma cell lines. *Cancer Res.* 52, 6188–6193.
- Muller, R.H., Maaßen, S., Weyhers, H., Specht, F., Lucks, J.S., 1996. Cytotoxicity of magnetite-loaded polylactide, polylactide/glycolide particles and solid lipid nanoparticles. *Int. J. Pharm.* 138, 85–94.
- Muller, R.H., Ruhl, D., Runge, S., Schulze-Forster, K., Mehnert, W., 1997. Cytotoxicity of solid lipid nanoparticles as a function of the lipid matrix and the surfactant. *Pharm. Res.* 14, 458–462.
- Olbrich, C., Bakowsky, U., Lehr, C.M., Müller, R.H., Kneuer, C., 2001. Cationic solid-lipid nanoparticles can efficiently bind and transfect plasmid DNA. *J. Control. Release* 77, 345–355.
- Phillips, A.D., Gonsalvi, L., Romerosa, A., Vizza, F., Peruzzini, M., 2004. Coordination chemistry of 1,3,5-triaza-7-phosphaadamantane (PTA): transition metal complexes and related catalytic, medicinal and photoluminescent applications. *Coord. Chem. Rev.* 248, 955–993.
- Schubert, M.A., Muller-Goymann, C.C., 2005. Characterization of surface-modified solid lipid nanoparticles (SLN): influence of lecithin and nonionic emulsifier. *Eur. J. Pharm. Biopharm.* 61, 77–86.
- Svilenov, H., Tzachev, C., 2014. Solid lipid nanoparticles—a promising drug delivery system. In: Seifalian, A., de Mel, A., Kalaskar, D.M. (Eds.), *Nanomedicine*. One Central Press, Manchester, pp. 187–237.
- Soussan, E., Cassel, S., Blanzat, M., Rico-Lattes, I., 2009. Drug delivery by soft matter: matrix and vesicular. *Angew. Chem. Int. Ed.* 48, 274–288.
- Souto, E., Doktorovova, S., Gonzalez-Mira, E., Egea, M., Garcia, M., 2010. Feasibility of lipid nanoparticles for ocular delivery of anti-inflammatory drugs. *Curr. Eye Res.* 35, 537–552.
- Sternberg, B., Sorgi, F.L., Huang, L., 1994. New structures in complex formation between DNA and cationic liposomes visualized by freeze-fracture electron microscopy. *FEBS Lett.* 356, 361–366.
- Tabatt, K., Sameti, M., Olbrich, C., Muller, R.H., Lehr, C.M., 2004. Effect of cationic lipid and matrix lipid composition on solid lipid nanoparticles-mediated gene transfer. *Eur. J. Pharm. Biopharm.* 57, 155–162.
- Vighi, E., Montanari, M., Hanuskova, M., Iannucelli, V., Coppi, G., Leo, E., 2012. Design flexibility influencing the *in vitro* behavior of cationic SLN as a nonviral gene vector. *Int. J. Pharm.* 12, 10–13.
- Wheate, N.J., Collins, J.G., 2003. Multi-nuclear platinum complexes as anti-cancer drugs. *Coord. Chem. Rev.* 241, 133–145.

618
619
620
621
622
623
624
625
626
627
628
629
630
631
632
633
634
635
636
637
638
639
640
641
642
643
644
645
646